J. Astrophys. Astr. (2006) **27,** 339–346

Study of Microflares through SOXS Mission

Rajmal Jain[1,*], Vishal Joshi[1], Yoichiro Hanaoka[2], T. Sakurai[2] & Nipa Upadhyay[3]
[1]*Physical Research Laboratory, Navrangpura, Ahmedabad 380 009, India.*
[2]*National Astronomical Observatory of Japan (NAOJ), Mitaka, Tokyo, Japan.*
[3]*C. U. Shah Science College, Ashram Road, Ahmedabad 380 014, India.*
[*]*e-mail: rajmal@prl.res.in*

Abstract. We present a study of 10 microflares observed in 4–30 keV by SOXS mission simultaneously with Hα observations made at NAOJ, Japan during the interval between February and August 2004. The X-ray and Hα light curves showed that the lifetime of microflares varies between 4 and 25 min. We found that the X-ray emission in all microflares under study in the dynamic energy range of 4–30 keV can be fitted by thermal plus non-thermal components. The thermal spectrum appeared to start from almost 4 keV, low level discriminator (LLD) of both Si and CZT detectors, however it ends below 8 keV. We also observed the Fe line complex features at 6.7 keV in some microflares and attempted to fit this line by isothermal temperature assumption. The temperature of isothermal plasma of microflares varies in the range between 8.6 and 10.1 MK while emission measure between 0.5 and 2×10^{49} cm^{-3}. Non-thermal (NT) emission appeared in the energy range 7–15 keV with exponent $-6.8 \leq \gamma \leq -4.8$. Our study of microflares that had occurred on 25 February 2004 showed that sometimes a given active region produces recurrent microflare activity of a similar nature. We concluded from X-ray and simultaneous Hα observations that the microflares are perhaps the result of the interaction of low lying loops. It appears that the electrons that accelerated during reconnection heat the ambient coronal plasma as well as interact with material while moving down along the loops and thereby produce Hα bright kernels.

Key words. X-ray detectors—coronal 100 ps—solar flares—microflares —hard X-ray emission.

1. Introduction

Hard X-rays (> 20 keV) were discovered with a balloon-borne instrumentation to occur on an average once every ~ 6 min near solar maximum (Lin *et al.* 1984). This investigation considered that the energy released in accelerated electrons, summed over HXR bursts of all sizes, might contribute significantly to the heating of the active corona. Recently, Lin *et al.* (2001) investigated HXR microflares up to 8 keV using BATSE/CGRO detectors. They found that the generally steep HXR spectra (power-law fits with exponent 3–7) reveal that most of the flare energy is in the non-thermal

electrons at lowest energy. Furthermore, the similarity between the distributions of frequency *vs.* energy release for > 8 keV bursts and the active region transient brightening (ARTBs) seen in soft X-rays by the SXT/YOHKOH instrument (Shimuzu 1995) suggested that these accelerated electrons may provide the energy for ARTBs. Recently Liu *et al.* (2004) have reported that microflares are seen in Hα, soft and hard X-ray wavelengths and their temporal evolution resembles large flares. They found that these small impulsive microflare events are located near well-defined magnetic neutral lines in active regions. The X-ray spectral analysis of the microflares and their association with type III radio bursts could enable them to conclude that the X-rays over 10 keV are emitted by non-thermal electrons.

Sylwester *et al.* (2000) used gas filled proportional detectors to improve sensitivity and spectral resolution in the energy band 2 keV to 8 keV, which, however, revealed FWHM > 1 keV at 5.9 keV, but succeeded in observing microflares. RHESSI (Lin *et al.* 2002) uses germanium detectors to achieve this goal by cooling them to < 75K in order to reduce the dark counts (noise) significantly. On the contrary, our SOXS payload (Jain *et al.* 2005) employs near-room temperature Si and CZT diodes, which operate between -5 and -30°C with the help of thermoelectric cooler coupled with the detector itself. These detectors (Jain *et al.* 2000, 2002a, b) provide high sensitivity for handling a large number of counts and high spectral resolution (sub-keV at < 10 keV). These features of the detectors however, enabled us to observe the X-ray emission from microflares to major flares as a full disk integrated contribution. Thus, in order to study the contribution from individual microflares we have to observe them during the passage of a single active region on the solar disk. Jain *et al.* (2005) described in detail the potential use of SOXS mission to study the microflares.

In this paper, we study microflares using temporal and spectra data from the Si and CZT detectors of the SOXS mission. We aim to address the question of whether the non-thermal nature of microflares extends below 10 keV, currently known as low energy cut-off limit for hard X-ray emission, and whether thermal emission also contributes to the microflares.

2. Observations

Flares on GOES intensity class $\leq$ C1.0 are defined as microflares (Chang *et al.* 2004). We also adopt this definition to identify the microflares. Kumar (2004) studied the statistical relationship between SOXS and GOES flares as both missions are in geostationary orbit and both measure full disk integrated X-ray emission. He found correlation coefficient 0.9 between flares observed by these two missions. The best fit of correlation was presented by Kumar (2004) in the form of the following empirical relation:

$$\text{Log [SOXS flux (Y)]} = \text{A} + \text{B}^{*} \log \text{[GOES flux (X)]}, \tag{1}$$

where SOXS flux is in counts/s and GOES flux is in watts/m^2. Based on the study of a large sample of flares, Kumar (2004) derived A and B for Si and CZT detectors of SOXS for 7–10 keV energy band as the following:

For Si:

$$\text{A} = 8.07,$$

$$\text{B} = 1.12,$$

Table 1. List of SOXS microflares under investigation.

Sl. no.	Date	Time(UT) Begin	Peak	End	Peak int. 7–10 keV CZT	GOES class	Hα class	Location	NOAA region no.
1	25 Feb 04	04:07:53	04:09:24	04:15:03	17	B5.5	Sf	N13W03	10564
2	25 Feb 04	04:15:03	04:17:06	04:22:04	20	B8.9	Sf	N13W03	10564
3	25 Feb 04	04:24:03	04:25:25	04:29:18	15	B9.2	Sf	N13W03	10564
4	25 Feb 04	05:02:23	05:06:35	05:22:14	30	B9.8	Sf	N14W03	10564
5	25 Feb 04	05:22:14	05:27:06	05:31:58	22	C1.0	Sf	N13W03	10564
6	25 Feb 04	06:45:58	06:51:18	06:56:20	26	C1.0	Sf	N13W03	10564
7	01 May 04	04:33:31	04:43:39	04:58:00	16	B8.9	Sf	S10W25	10601
8	22 Jun 04	05:20:23	05:22:03	05:24:05	34	B8.1	Sf	S13W15	10635
9	09 Aug 04	04:06:39	04:12:43	04:18:58	23	B9.2	Sf	S12E45	10656
10	09 Aug 04	04:18:58	04:25:24	04:31:50	19	B8.2	Sf	S12E45	10656

and for CZT:

$$A = 6.77,$$

$$B = 0.844.$$

The above study enabled Kumar (2004) to define the higher threshold level of microflares for example in CZT detector to set at 60 count/s, i.e., C1 in GOES class. Thus while selecting the microflares for our current study we chose only those flares as microflares, which have been observed by SOXS under the above definition plus either in GOES or in Hα. In Table 1, we show the list of microflares observed by SOXS mission and analysed by us together with their details in GOES and Hα wavebands. A total of 10 microflares observed by Si and CZT detector of SOXS mission between February and August 2004 were considered for our detailed study. The Hα observations were made at National Astronomical Observatory of Japan (NAOJ), Mitaka, simultaneous to the SOXS mission. The seeing was average between 1 and 2 arcsec during all Hα observations.

3. Analysis and results

Details of the SOXS mission, in-flight performance, calibration, instrumental response and background are described by Jain *et al.* (2005). The data format and data analysis techniques are also presented by him. SOXS delivers two types of data, viz., temporal and spectral mode. In the temporal mode CZT detector provides light curve in 6–7, 7–10, 10–20, 20–30 and 30–56 keV energy bands. The microflare in any of these energy bands is identified if its signal is $\geq 3\sigma$ than the background in the respective energy band. After unambiguous identification of the microflare it is cross-correlated with GOES and/or Hα observations on time and intensity scales. Then we undertake detailed spectra analysis for the period of microflare using standard SOXS software – SOXSoft (Patel and Jain 2005). In Fig. 1, we show the light curve of the microflares

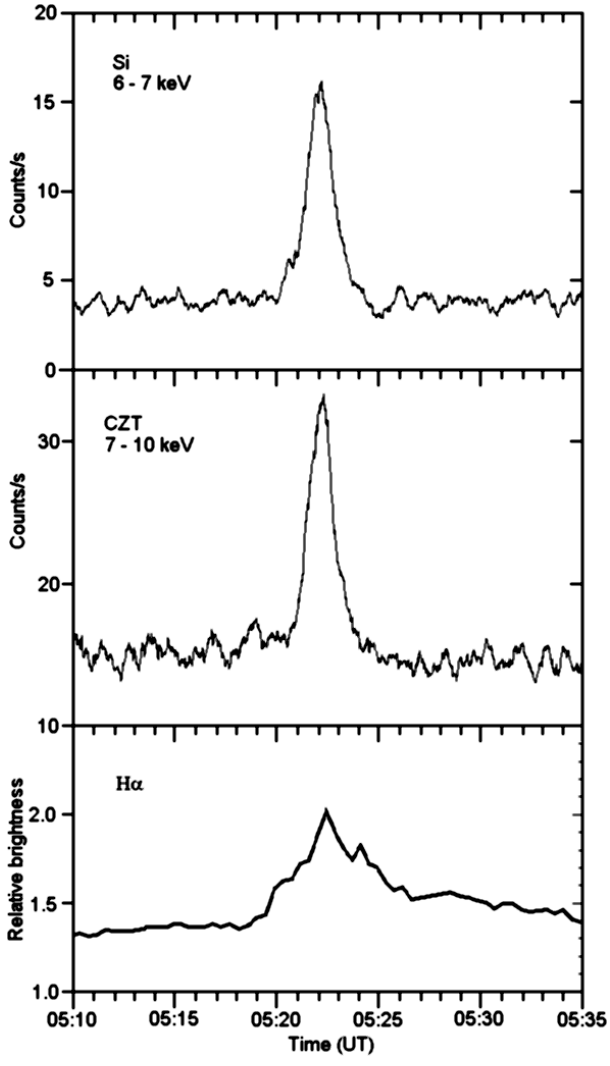

Figure 1. Light curves of 22 June 2004 microflare. **Top and middle panels:** X-ray emission in 6–7 and 7–10 keV as seen by Si and CZT detectors of SOXS mission respectively as a function of time. **Bottom panel:** variation Hα relative brightness over the same time interval.

observed on 25 February 2004 in 6–7 and 7–10 keV energy bands by Si and CZT detectors respectively. Also shown in the bottom panel is the light curve of Hα relative brightness. In Fig. 2, we show Hα filtergrams of the typical microflare observed on 22 June 2004. It may be noted that the two bright kernels are the foot points of the bright loop connecting them. We observed the loop-like structure in the images before the flare, thus apparently the loop-like structure is a part of the pre-existing plage. The brightness of the loop-like structure increased a little bit during the flare, but the increase of the brightness of the kernels was much more remarkable. The six images in Fig. 2 show a remarkable change of brightness of the loop as well as of the kernels. The light curves enabled us to estimate the lifetime of each microflare. We

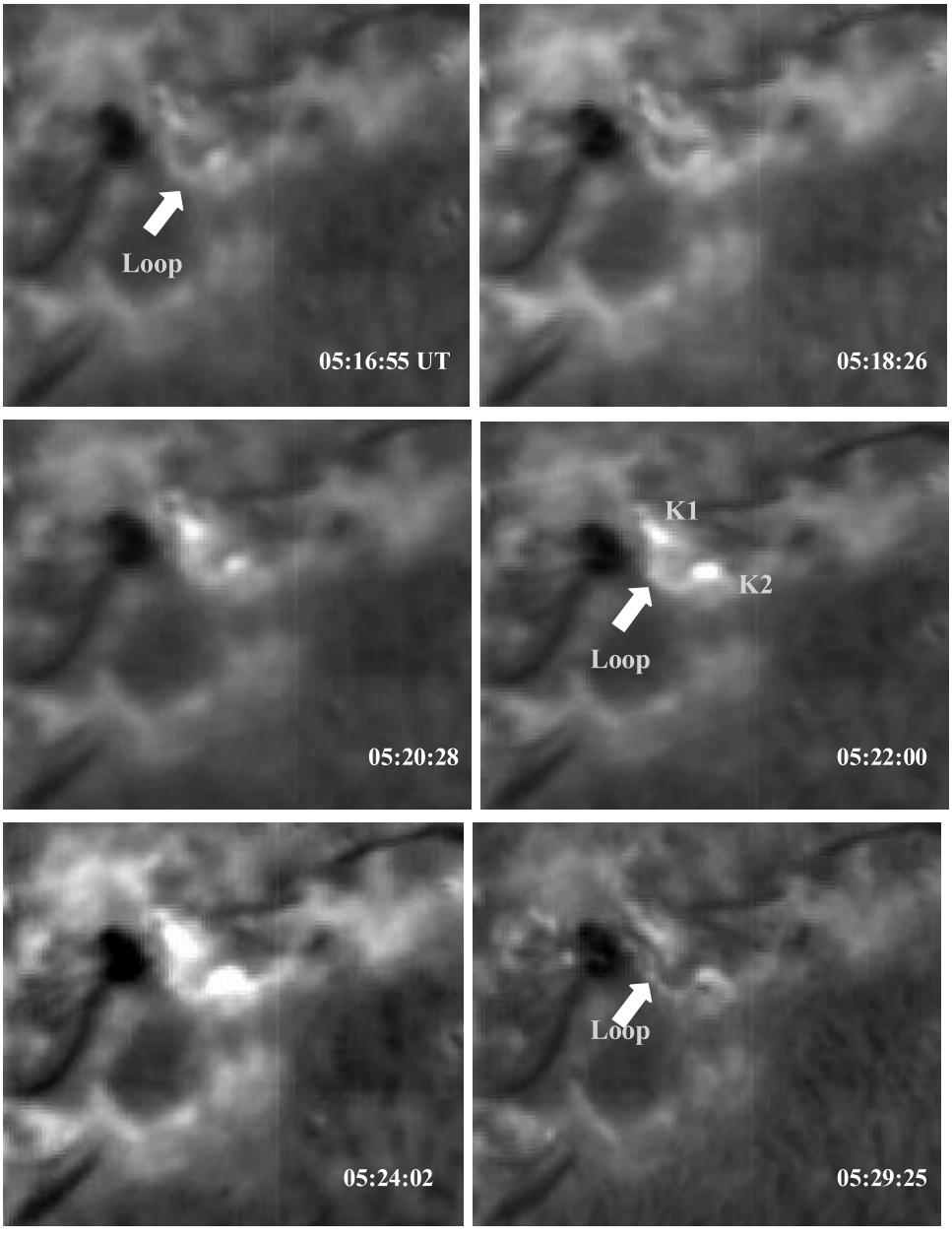

Figure 2. Hα filtergrams of 22 June 2004 flare. Two bright kernels K1 and K2 connected by a small bright loop, as shown in the filtergram at 05:22:00 UT, may be noted. The loop and the kernels fade out during the decay phase.

found that it varies between 4 and 25 min. In Hα these microflares are classified as of Sf importance.

We have carried out a detailed analysis of the X-ray photon spectra of each flare. In Fig. 3, we have shown Si and CZT detectors photon spectra of 22 June 2004

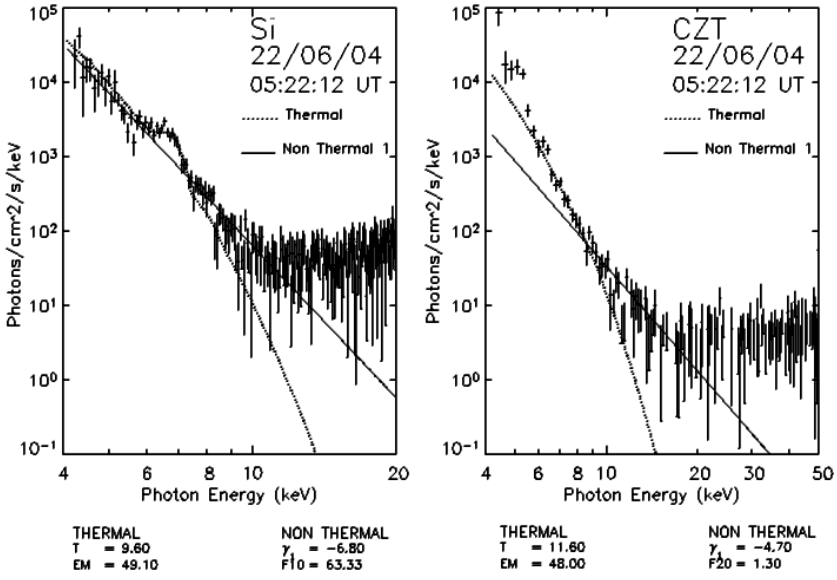

Figure 3. X-ray photon spectra of 22 June 2004 microflare as seen by Si and CZT detectors. The observed photon flux at every channel is represented by $\pm 1\sigma$ error. In Si spectra Fe line complex at 6.7 keV may be noted. CZT shows only continuum X-ray spectrum. Thermal and non-thermal fit is presented for spectra from both detectors. Si detector shows X-ray photon spectrum for the microflare up to 15 keV while CZT up to 25 keV.

microflare that occurred at 05:22:12 UT. The photon spectra are fitted with thermal and non-thermal components. It may be noted from the figure that the photon spectra of this microflare reveal Fe line complex at 6.7 keV. However, Fe/Ni line complex is not visible. On the other hand, our analysis showed that each microflare does not exhibit Fe line complex, which otherwise is observed in all higher important class flares (Jain *et al.* 2005). The isothermal plasma emission was considered to fit the X-ray emission below 10 keV including Fe line complex but we found that the contribution of thermal component was valid below 8 keV in all microflares under study. The thermal spectrum appeared to start from almost 4 keV, i.e., low level discriminator (LLD) of both Si and CZT detectors, however, it ends around 8 keV. The temperature of the isothermal plasma of microflares varies in the range between 8.6 and 10.1 MK while emission measures between 0.5 and 2×10^{49} cm^{-3} for different microflares studied in this investigation. The non-thermal component was found to begin from 7 keV, and therefore power-law fit between 7 and 14 keV was more appropriate. However, the photon index (exponent) γ varies as $-6.8 \leq \gamma \leq -4.8$ among different microflares.

4. Discussion

A series of microflare activity may be noted from Table 1 in the NOAA active region no. 10564 on 25 February 2004. This active region produced recurrent microflare activity. Almost all microflares produced by this region showed an almost similar kind of X-ray photon spectrum indicating that a single type of energy release mechanism was operating all over the active region. Hα filtergrams of the active region

under study revealed that either a thin filament channel or small filament showed considerable activity preceding each microflare. This indicates that microflares are perhaps the result of the interaction of low lying loops. It appears that the electrons accelerated during reconnection caused by the interaction of the low lying loops heat the ambient coronal plasma as well as interact with material while moving down along the loops. The heated coronal plasma produced soft X-ray emission as revealed in the X-ray photon spectrum between 4 and 8 keV including Fe line complex. These accelerated electrons when interacted with chromosphere produced Hα bright kernels as shown in Fig. 2. The X-ray photon spectra between 7 and 14 keV showed non-thermal component. We conclude from X-ray photon spectra and simultaneous Hα filtergrams that thermal and non-thermal mechanisms are operating in the microflares in agreement with Benz & Grigis (2002); Krucker *et al.* (2002) and Liu *et al.* (2004). The other possibility of microflare occurrence through reconnection of the higher altitude coronal loops and there by accelerated electrons which could heat the plasma at the intersection region of the separatrices of the active region cannot be ignored.

5. Conclusion

We analyzed 10 microflares for the current study and found that the X-ray photon spectra below 8 keV are of thermal nature, while above 8 keV are of non-thermal nature. We conclude that the non-thermal electrons accelerated at the loop apex move along such low lying coronal loops and interact with chromospheric material at the foot points and produce Hα bright kernels. The thermal electrons produce soft X-ray emission observed by GOES and SOXS mission in low energy bands.

References

Benz, A. O., Grigis, P. 2002, *Solar Phys.*, **210**, 431.

Chang, L., Jiong, Q., Gary, D. E., Krucker, S., Wang, H. 2004, *ApJ*, **604**, 442.

Jain, Rajmal, Deshpande, M. R., Dave, H. H., Manian, K. S. B., Vadher, N. M., Shah, A. B., Ubale, G. P., Mecwan, G. A., Trivedi, J. M., Solanki, C. M., Shah, V. M., Patel, V. D., Kayasth, S. L., Sharma, M. R., Umapathy, C. N., Kulkarni, R., Kumar, Jain, A. K., Sreekumar, P. 2000, Technical Document – "*GSAT-2 Spacecraft – Preliminary Design Review (PDR) Document for Solar X-ray Spectrometer*", ISRO-ISAC-GSAT-2-RR-0155.

Jain, Rajmal, Dave, H. H., Vadher, N. M., Shah, A. B., Ubale, G. P., Shah, V. M., Solanki, C. M., Kayasth, S. L., Patel, V. D., Shah, K. J., Deshpande, M. R. 2002a, PRL Technical Document "*Characterization and Response of Si PIN and CZT Detectors*", PRL-GSAT-2-SOXS-0180.

Jain, Rajmal, Dave, H. H., Vadher, N. M., Shah, A. B., Ubale, G. P., Shah, V. M., Solanki, C. M., Kayasth, S. L., Patel, V. D., Pabari, Jayesh, Shah, K. J., Panchal, G. A., Deshpande, M. R. 2002b, PRL Technical Document "*Configuration Design Review (CDR) Document of SOXS Low Energy Detector (SLED) Package*", PRL-GSAT-2-SOXS-0181.

Jain, Rajmal, Dave, Hemant, Shah, A. B., Vadher, N. M., Shah, Vishal M., Ubale, G. P., Manian, K. S. B., Solanki, Chirag M., Shah, K. J., Kumar, Sumit, Kayasth, S. L., Patel, V. D., Trivedi, Jayshree, J., Deshpande, M. R. 2005, *Solar Phys.*, **227**, 89.

Krucker, S., Christe, S., Lin, R. P., Hurford, G. J., Schwartz, R. A. 2002, *Solar Phys.*, **210**, 445.

Kumar, Sumit 2004, M. Tech thesis, Andhra University, Hyderabad, India.

Lin, R. P., Schwartz, R. A., Kane, S. R., Feffer, P. T., Hurley, K. C. 1984, *ApJ*, **283**, 421.

Lin, R. P., Feffer, P. T., Schwartz, R. A. 2001, *ApJ*, **557**, L125.

Lin, R. P. *et al.* 2002, *Solar Phys.*, **210**, 3.
Liu, C., Qiu, J., Gary, D. E., Nita G. M., Wang, H. 2004, *ApJ*, **612**, 530.
Patel, Falgun and Jain, Noopur 2005, SOXS/PRL Technical document, "Software Development for data Processing and Analysis of Data from Solar X-ray Spectrometer (SOXS) Mission Onboard GSAT-2 Spacecraft".
Shimuzu, T. 1995, *Publ. Astron. Soc. Japan*, **47**, 251.
Sylwester, J., Farnik, F., Likin, O., Kordylewski, Z., Siarkowski, M., Nowak, S., Piocieniak, S., Trazebinsk, W. 2000, *Solar Phys.*, **197**, 337.